



Design of a Flexible Bionic Ankle Prosthesis Based on Subject-specific Modeling of the Human Musculoskeletal System

Jianqiao Jin¹ · Kunyang Wang^{1,2} · Lei Ren^{1,2,3} · Zhihui Qian¹ · Wei Liang¹ · Xiaohan Xu¹ · Shun Zhao¹ · Xuewei Lu³ · Di Zhao¹ · Xu Wang¹ · Luquan Ren^{1,2}

Received: 24 October 2022 / Revised: 5 December 2022 / Accepted: 8 December 2022 / Published online: 24 December 2022
© The Author(s) 2022

Abstract

A variety of prosthetic ankles have been successfully developed to reproduce the locomotor ability for lower limb amputees in daily lives. However, they have not been shown to sufficiently improve the natural gait mechanics commonly observed in comparison to the able-bodied, perhaps due to over-simplified designs of functional musculoskeletal structures in prostheses. In this study, a flexible bionic ankle prosthesis with joints covered by soft material inclusions is developed on the basis of the human musculoskeletal system. First, the healthy side ankle–foot bones of a below-knee amputee were reconstructed by CT imaging. Three types of polyurethane rubber material configurations were then designed to mimic the soft tissues around the human ankle, providing stability and flexibility. Finite element simulations were conducted to determine the proper design of the rubber materials, evaluate the ankle stiffness under different external conditions, and calculate the rotation axes of the ankle during walking. The results showed that the bionic ankle had variable stiffness properties and could adapt to various road surfaces. It also had rotation axes similar to that of the human ankle, thus restoring the function of the talocrural and subtalar joints. The inclination and deviation angles of the talocrural axis, 86.2° and 75.1°, respectively, as well as the angles of the subtalar axis, 40.1° and 29.9°, were consistent with the literature. Finally, dynamic characteristics were investigated by gait measurements on the same subject, and the flexible bionic ankle prosthesis demonstrated natural gait mechanics during walking in terms of ankle angles and moments.

Keywords Ankle prosthesis · Bionic design · Soft materials · Variable stiffness · Gait mechanics

1 Introduction

The ankle–foot complex plays a very important role in human daily activities. For people with amputation (i.e., amputees), physical defects of foot or ankle can have a great impact on their daily lives. One study found that approximately 1.6 million people underwent amputation in the USA in 2005, or 1 person for every 190 Americans [1]. Statistical

analysis approximately predicts that the number of amputees in the USA will continue to increase by approximately 2 million by 2050 [1]. Therefore, how to actively prevent the further increase in this number and provide more functional prosthetic products for the existing amputees requires further efforts in the field [1, 2].

Transtibial (below-knee) amputation is a common type of amputation typically resulting from severe injuries, infections or diseases. Ankle prostheses are widely used to replace the below-knee amputee's limbs to reproduce the functional mobility [3]. Currently, the most conventional ankle prostheses are the rigid prostheses in which the motions are achieved by traditional hinge joints or bearings [3–5]. Although these prostheses can well support body weight, absorb shock, and achieve high work efficiency during locomotion, they cannot simulate the natural gait mechanics of the healthy human body [3]. Most of them contain over-simplified mechanical structures with only one or two degrees of freedom (DoFs), which is totally different

✉ Kunyang Wang
kywang@jlu.edu.cn

✉ Lei Ren
lren@jlu.edu.cn

¹ Key Laboratory of Bionic Engineering, Ministry of Education, Jilin University, Changchun 130025, China

² Weihai Institute for Bionics, Jilin University, Weihai 264402, China

³ School of Mechanical, Aerospace and Civil Engineering, University of Manchester, Manchester M13 9PL, UK

from the six DoFs in three planes of the anatomical ankle. In addition, high weight of rigid parts also increases the metabolic cost of human locomotion, which ultimately leads to undesired changes in the natural gait characteristics of the amputees and secondary damages to their healthy joints.

On this basis, some researchers have proposed that passive compliant prostheses could be used to improve the rigid mechanism prostheses. Compared with rigid prostheses, flexible passive prostheses are applicable to provide a wider range of motions, and their lower weight as well as more human-like mechanism features increase their use stability [6–9]. Meanwhile, due to the adaptability of soft materials, flexible prostheses have more DoFs and thus can adapt to different road conditions by better mimicking the healthy ankle joints [5, 10, 11]. For example, Nguyen et al. [9] proposed a flexible prosthesis made of glass fiber composite materials (GFRP) that optimized the overall configuration using Finite Element (FE) methods. The features of the ankle joint and foot were constructed using a simplified method of one-piece formation. Another passive prosthesis called multi-axis compliant prosthetic ankle foot (MACPA) [12, 13] was developed, consisting of an upper and lower part with a hinge mechanism on the upper part to allow the limb to turn in or out. The lower part used soft materials for integrated design, aiming to realize energy storage and release for assisting walking through self-deformation of elastic materials. Sam et al. [14, 15] developed a passive prosthesis with flexible elements on the basis of the gait characteristics of human walking.

However, the flexible passive prostheses introduced above only performed some functional improvements over rigid prostheses in terms of production cost and weight, but they were still poor at restoring the natural motions during walking of the healthy ankle-foot in a more comprehensive way. To resolve this problem, a prosthesis called SoftFoot [16] was developed through bionic exploration of human foot. The functions of the plantar joint and plantar fascia were incorporated into the design, which greatly improved the prosthesis flexibility. SoftFoot can not only adapt to more irregular road surfaces, but also to the configuration of the plantar fascia, which reduces the metabolic consumption of the amputee. However, this prosthesis cannot effectively simulate the natural gait mechanics of the human ankle joint [17]. Schlafly et al. [18] designed a prosthesis called CAPA (compliant and articulated prosthetic ankle) based on the ability of the human ankle to support the body and adapt to different terrains. However, only a few breakthroughs in basic theory have been made in the research of flexible prostheses, and they can only partly ensure walking performance because of the inherent limitations of soft materials [19–22].

Consequently, this study develops a flexible bionic ankle prosthesis based on customized modeling on the musculo-skeletal system of a below-knee amputee's healthy ankle.

Ankle bones of tibia–fibula, talus, and calcaneus were reconstructed as the rigid parts of the prosthesis, forming two functional joints (talocrural and subtalar). Three types of soft material-based inclusions with different outer profiles were designed to mimic the soft tissues around the human ankle, providing both stability and flexibility during different phases of walking. Polyurethane rubber was used as the covering soft material due to its excellent mechanical properties and stable chemical structure. FE simulations under 70 time instants walking conditions were then conducted to find the best profiles of the soft material inclusions. Then, the stiffness of the bionic ankle under various working conditions and the rotation axes during walking were studied by separate FE analysis. Finally, gait measurements were conducted on the same amputee wearing the flexible ankle prosthesis. Gait mechanics were compared between the prosthetic side and the healthy side. We hope that this study could in part provide creativity and design inspiration for the development of flexible ankle prostheses.

2 Materials and Methods

2.1 Human Ankle–foot Reconstruction

Ankle–foot bone images of the healthy (left) side of a below-knee amputee (age: 27 years, weight: 77 kg; height: 182 cm; no history of lower extremity diseases on the healthy side) were obtained by a GE Revolution CT scanner (General Electric, USA) at 0.624 mm slice intervals. The subject provided prior written informed consent before participating in the CT scanning and gait measurements. Each image had dimensions of 512×512 pixels and represented a slice in the sagittal plane of the human body (Fig. 1a). A surface model was then rebuilt and smoothed in Mimics (Materialize NV, Belgium) and mirrored to a solid right ankle–foot model (Fig. 1a) in SolidWorks (Dassault System, USA). This study was approved by the Ethics Committee of the Second Hospital of Jilin University (Log# 2,021,072), in accordance with the Declaration of Helsinki (2013) and Biomedical Research Involving Human Subjects International Code of Ethics for Research (2002).

2.2 Design of the Bionic Ankle Prosthesis

In this study, three types of soft material inclusions (Fig. 1b) were designed to imitate the soft tissues surrounding the human ankle, providing stability and adaptability during walking. To facilitate comparative analysis and eliminate uncertain factors, the internal structure designs of the three inclusions were consistent. The specific method of modeling was to carry out regular processing according to the well-positioned foot bone parts, set each part of the foot bone

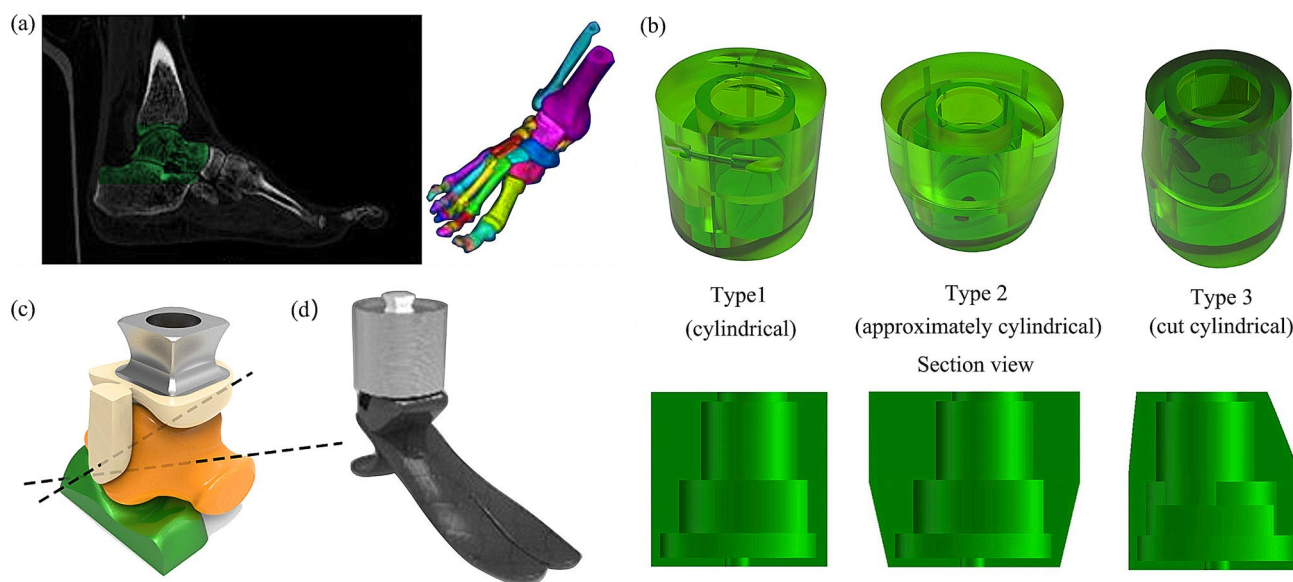


Fig. 1 Design of the ankle prosthesis inspired by the human ankle–foot complex. **a** Acquisition of the ankle–foot model. **b** Three soft material inclusions. **c** Prosthetic ankle design. **d** 3D rendering of the prosthesis

according to the ellipse, and pull out the mold to stretch out the entity to form the internal configuration of inclusion. For the external shape, according to the characteristics of the human leg, the shape of the type 1 inclusion was assumed as a regular configuration (cylindrical). Type 2 inclusion was divided into upper and lower parts in which the shape of the internal and external condyles was the boundary (approximately cylindrical). As the upper half considered as the main part to perform relatively large movements of plantar flexion and dorsiflexion, the outer profiles were thickened. Meanwhile, the thickness of the regular configuration in the lower half was reduced. For the type 3 inclusion, considering the better supporting deformation of the soft materials, the thickness of the type 1 inclusion was too large. As a result, according to the human bone profiles, the outer profiles of the type 3 inclusion were obtained by removing the extra area (by a cylindrical cut). Polyurethane rubber was selected as the soft material for all three types because of its favorable mechanical properties and stable chemical structure [20, 22].

For the rigid parts of the ankle prosthesis, talus and calcaneus were kept as original, tibia and fibula were constructed as a whole (i.e., tibiofibular), leg tube connectors were placed at the top of the integrated tibiofibular part, and all parts of the ankle bones were scaled in proportion (Fig. 1c). The ankle model parts processed were then imported into a 3D printer, Stratasys J850 (Stratasys, USA), to produce the physical prototype of talus, calcaneus, tibiofibular, and tube connectors. The foot plate was derived from the profiles of human foot bones and simplified as a 4-mm curved plate. The human foot arch has great mechanical characteristics in

terms of shock absorption and stability [23]. To better simulate the gait movement of the human body, the foot plate in this study takes the role of the human arch into consideration. The foot plate was made of commercial carbon fiber to provide adequate strength and reduce the overall weight. To suitably limit the movements of the soft material inclusions and make the connection with the foot plate more stable, the prosthetic ankle was covered by a metal shell (Fig. 1d).

2.3 Finite Element Analysis

Three types of FE simulations were carried out in this study to select the appropriate type of soft material inclusions, analyze the 3D ankle stiffness of the prosthesis under different working conditions, and calculate the rotation axis of the prosthetic ankle during a normal walking gait. A 3D FE model (Fig. 1c and d) containing tibiofibular, talus, calcaneus, leg connectors, soft material inclusions, and foot plate was developed in Abaqus CAE (Simulia, USA). All parts were modeled using high-quality tetrahedral mesh elements (C3D4), and corresponding material parameters (elastic modulus and Poisson's ratio) [24] were assigned to different components (Table 1). It should be noted that the rigid part here is the metal shell surrounding the bionic prosthetic ankle (not leg connector), which is used to fix and wrap the polyurethane materials. Tie constraints were applied to connect the tibiofibular to the leg connector and form the calcaneus, or the soft inclusion into the foot plate. Frictionless sliding contacts were defined between the interface of bone to bone and bone to soft material inclusions.

Table 1 Mesh quantity and material properties of the prosthetic components

Components	Soft material	Foot bone [23]	Rigid parts	Foot plate [24]
Mesh quantity	34,527	43,624	16,864	58,649
Young's modulus [MPa]	7.8	7300	210,000	17,000
Poisson's ratio	0.47	0.3	0.3	0.1

To select the proper type of soft inclusions with minimum principal stress, a kinematic simulation was conducted during the stance phase of walking gait for all three types of designs. The stance phase was divided into 70 time instants, and the kinematic simulation was conducted at each instant. The ground reactions at each instant were defined according to the literature [17]. To investigate the 3D ankle stiffness of the prosthesis, 12 different working conditions were defined based on the compression test setups [25]. A vertical force of 400 N was applied to obtain the stress and displacement values under each condition. The deformation of the prosthetic ankle and the moment around the ankle were then calculated to quantify the ankle stiffness at each condition. To calculate the rotation axis of the prosthetic ankle during walking, the local bone coordinate system was defined for the tibiofibular, talus and calcaneus. The relative 3D transformations between these bones were calculated for all the 70 time instant stance phases of normal walking. The input parameters for each simulation mainly included the angle between the foot and the ground as well as the ground reactions, which were derived from the literature [17, 26].

2.4 Joint Axis Calculation

To verify that the bionic ankle could restore the natural movements of a healthy human ankle, the walking gait of the prosthesis was simulated in Abaqus. The rotation axis of the talocrural joint and the subtalar joint during walking was calculated using a helical axis approach [27] in the FE simulation. The joint axis was defined as the axis that best represented the rotation occurring between two articulating bone-like components during a defined time period from heel strike to toe off (talocrural: talus and tibia; subtalar: calcaneus and talus). The landmarks used to define the bone frame are shown in Table 2, and their coordinates at different time instants were obtained from the FE analysis. The talocrural or subtalar joint axis was described by a position vector and an orientation vector in the talus bone frame and then transformed to be described in the global foot frame.

Table 2 Landmarks used for joint axis calculations

Tibiofibula	Talus	Calcaneus
Medial malleolus (MM)	Medial tubercle (MT)	Upper ridge of the calcaneus (CA)
Lateral malleolus (LM)	Most lateral point (LP)	Most medial point (MS)
Front most point of the tibia (FT)	Front most point on the head (FH)	Lateral fibular trochlea (LF)

The orientation angles of the talocrural and subtalar joint axes, including deviation and inclination, were then calculated for comparison with the literature. All calculations were conducted by using MATLAB (MathWorks).

2.5 Gait Measurements

The subject was the amputee who participated in the human ankle-foot reconstruction by CT scanning. In the early stage, the experimental subjects were briefly introduced to the process and trained accordingly, which ensured the smooth progress of the experiment and the collection of relatively stable data. Wearing the flexible bionic ankle prosthesis, the subject walked on a 10-m sidewalk at three different self-selected speeds: slow (1.25 ± 0.27 m/s), normal (1.51 ± 0.32 m/s), and fast (1.82 ± 0.36 m/s). Each speed was measured 10 times to ensure representative walking data were recorded and used for all analyses. Kinematic data were collected at 100 Hz using a seven-infrared camera motion capture system (Vicon, UK), and ground reaction force/moment data were recorded at 1000 Hz using a three force-plate array (Kistler, Switzerland). To ensure experiment safety, handrails were placed on both sides of the passages of the three force measuring plates (the handrails were not reflective).

A group of specially designed thermoplastic plates [28] were attached to the six body segments (feet, shanks, thighs), each with a cluster of four reflective markers. The plastic plates reduced the relative movement between the markers on a segment, thereby improving the accuracy of the measured data [29, 30]. The anatomical landmarks were located from a series of static calibration procedures by using a calibration wand and reflective markers. The calibration markers were then removed before walking tests according to the calibrated anatomical system technique [31]. The joint centers were defined based on anatomical landmarks. Measured data were processed using customized MATLAB codes for 3D kinematic and kinetic analysis of general biomechanical multibody systems. The marker data were filtered using a

low-pass zero-lag fourth-order Butterworth digital filter with a cutoff frequency of 6.0 Hz.

2.6 Statistical Analysis

The results of gait measurement are shown as the mean \pm standard deviation ($n = 10$). Statistical significance was tested using ANOVA (single factor) by SPSS 25.0 software (IBM, USA). Probability values of $p < 0.05$ were considered statistically significant, and all data are presented at a $p < 0.05$ significance level unless otherwise stated.

3 Results

3.1 Structure Determination of the Soft Materials

By comparing the displacement and stress distribution of three polyurethane inclusions with different shapes (Fig. 2a and b), as well as the stress distribution of the prosthetic ankle bones (Fig. 2c) during walking, type 1 with cylindrical inclusions was finally chosen for the following analysis in this study. Fig. 2 was selected from the instant with the largest value in the 70 time-series simulation process, which was approximately between the middle and late stages of the stance phase. The results showed that the maximum displacement of the cylindrical polyurethane inclusions with a value of 1.08 mm was smaller than those of the other two types (type 2: 1.68 mm; type 3: 2.02 mm). Similarly, the maximum stress of the cylindrical polyurethane inclusions, 0.89 MPa, was smaller than those of the other two configurations (type 2: 2.60 MPa; type 3: 1.62 MPa). This indicates that the integral shape deformation and stress of the cylindrical polyurethane inclusions were the smallest, which could provide adequate stability during walking. For the internal bone, the maximum stress of the ankle joint surrounding the type 1 inclusions was 7.52 MPa, much smaller than those of the other two configurations with stresses of 12.61 MPa and 16.08 MPa, respectively. In conclusion, the flexible bionic prosthetic ankle using type 1 inclusions may offer better performance, durability and longer service life for walking.

3.2 3D Stiffness of the Ankle Prosthesis

To better explore the variable stiffness characteristics of the bionic ankle designed in this study, the prosthesis was placed in appropriate positions and simulated under compression. Four basic placements of the foot were used, namely, leaning backward (LB), forward (LF), medial (LM), and lateral (LL), resulting in a total of 12 different working conditions (4 uniaxial rotations and 8 biaxial rotations) as shown in Table 3.

In each condition, the stress and displacement were obtained (Fig. 3), and the stiffness of the bionic ankle was further analyzed (Fig. 4). The results showed that the bionic ankle prosthesis had different stiffnesses in each condition and could adapt to the needs of different road conditions. The maximum stress of the soft inclusions was 0.18 MPa for LB 40° and LL 40°, 83.3% larger than the minimum value of 0.03 MPa (appearing in the case of LB 40°). In addition, the maximum moments and rotation angles calculated under the 12 working conditions are listed in Table 4 and grouped for 3D stiffness analysis (Fig. 5).

Under the 12 working conditions, the minimum rotation angle in LF 40° and LL 40° (3.9°) was 31.6% lower than the maximum rotation angle (5.7°) in LB 40°. The maximum moment appeared at LF 40° (18.3 Nm) was 4.6% larger than the minimum moment appeared at LF 40° and LM 20° (17.5 Nm). Compared to the uniaxial rotations (Fig. 5a), the rotation angles of LB and LM were greater than those of LF and LL, respectively, and the rotation angles of LF were greater than those of LM. For the simulation of biaxial rotations, in the case of the same LB, the LM rotation angle value was greater than the LL value, consistent with the range of angle changes of the human ankle during walking [17, 18, 26]. Mechanical tests showed that the designed bionic prosthesis produced corresponding elastic deformation and moment under a specified bending force of 400 N, consistent with the variable stiffness characteristics of human walking under different conditions. This indicates that the prosthesis can potentially ensure dorsiflexion, plantar flexion, inversion and eversion gait comfort.

3.3 Joint Axis Rotations of the Ankle Prosthesis

The rotation axes of the talocrural joint and subtalar joint of the bionic prosthetic ankle were calculated based on the landmark coordinates recorded during walking (Fig. 6a and b), and then transformed into the global foot frame (Fig. 6c). The orientation angles of each axis were analyzed to compare with the literature data [32–35], as shown in Table 5. The results showed that the angle between the talocrural axis and the sagittal plane (TaloInc) was 86.2°, while the angle between the talocrural axis projected in the horizontal plane and the anterior–posterior axis of the sagittal plane (TaloDev) was 75.1°. The angle between the subtalar axis and the transverse plane (SubInc) was 40.1°, while the angle between the subtalar axis projected in the horizontal plane and the sagittal plane (SubDev) was 29.9°. These angles located in the range of able-bodied human ankles from the literatures. The bionic ankle with soft inclusions could successfully mimic the rotation axis of the human ankle during walking and restore the function of the talocrural and subtalar joints.

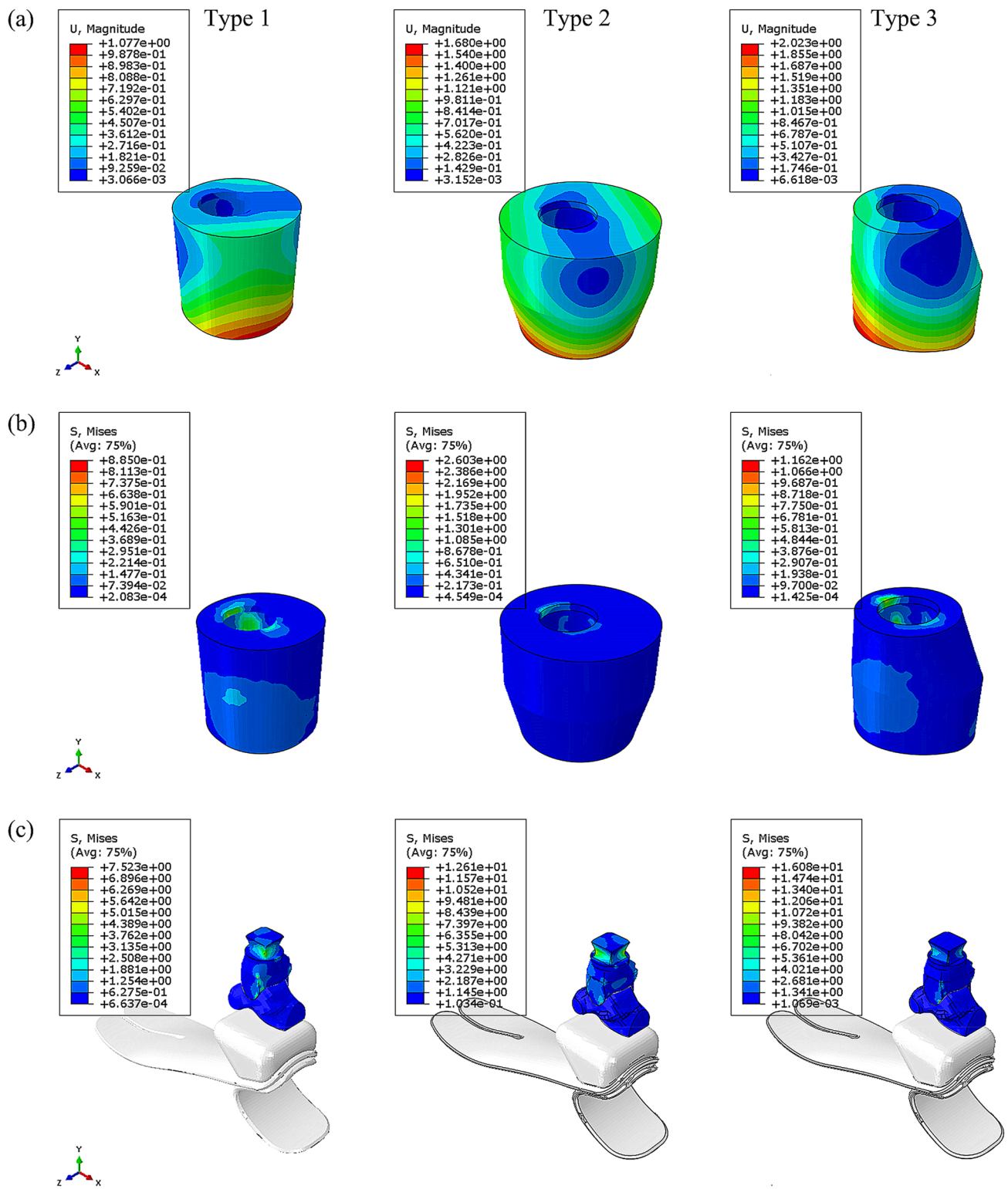


Fig. 2 Finite element analysis of three soft material inclusions. **a** Distribution of spatial displacement in the soft inclusions. **b** Distribution of maximum principal stress in the soft inclusions. **c** Distribution of maximum principal stress in the bones

Table 3 Twelve different working conditions of the prosthesis under compression

Conditions	1	2	3	4	5	6	7	8	9	10	11	12
LB	40°	/	/	/	40°	40°	40°	40°	/	/	/	/
LF	/	40°	/	/	/	/	/	/	40°	40°	40°	40°
LM	/	/	40°	/	20°	40°	/	/	20°	40°	/	/
LL	/	/	/	40°	/	/	20°	40°	/	/	20°	40°

LB leaning backward; LF leaning forward; LM leaning medial; LL leaning lateral. Each condition includes one or two placements

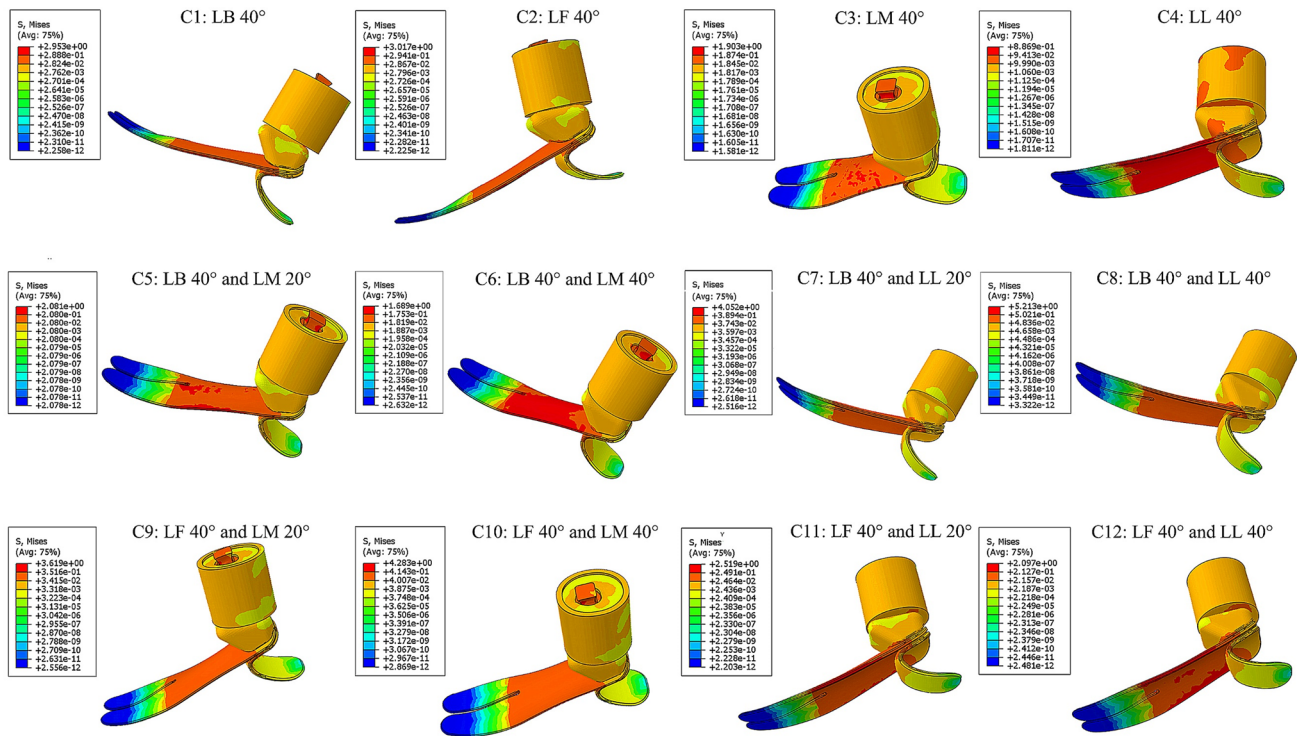


Fig. 3 Distribution of maximum principal stress in the prosthesis under different working conditions. C, abbreviation of the condition

3.4 Clinical Validation of the Ankle Prosthesis

The bionic ankle prosthesis was validated by the same amputee, for which the healthy side of ankle-foot bones were used as a design reference (Fig. 7). The ankles and moments of the prosthetic ankle in three planes (sagittal, coronal and transverse) were measured and analyzed under three different walking speeds (Fig. 8 and 9). These data were compared with their respective values in the three planes of the healthy side of the subject.

Generally, the trends of the ankle angles and moments in both the three planes of the prosthetic and healthy sides were similar. However, for the prosthetic ankle, the motion range in the transverse plane was smaller than that of the healthy side, while the angles in the sagittal plane were higher than that of the healthy side. Moreover, the time-angle curve of the ankle in the transverse plane was slightly shifted

forward relative to the healthy side. In addition, the peak ankle moments in all three planes were lower than those of the healthy side, except for the value in the sagittal plane at slow speed. Similar to the ankle angle, the time-moment curves of the ankle in all the planes were slightly shifted forward. With increasing walking speed, the peak moment in the sagittal plane of the prosthetic side gradually decreased, in contrast to the trend of the gait characteristics of the healthy side.

4 Discussion

In this study, a bionic prosthetic ankle was developed by extracting human ankle-foot bones and using suitable flexible materials to mimic the soft tissues around the human ankle. Soft material is useful in the overall simulation of

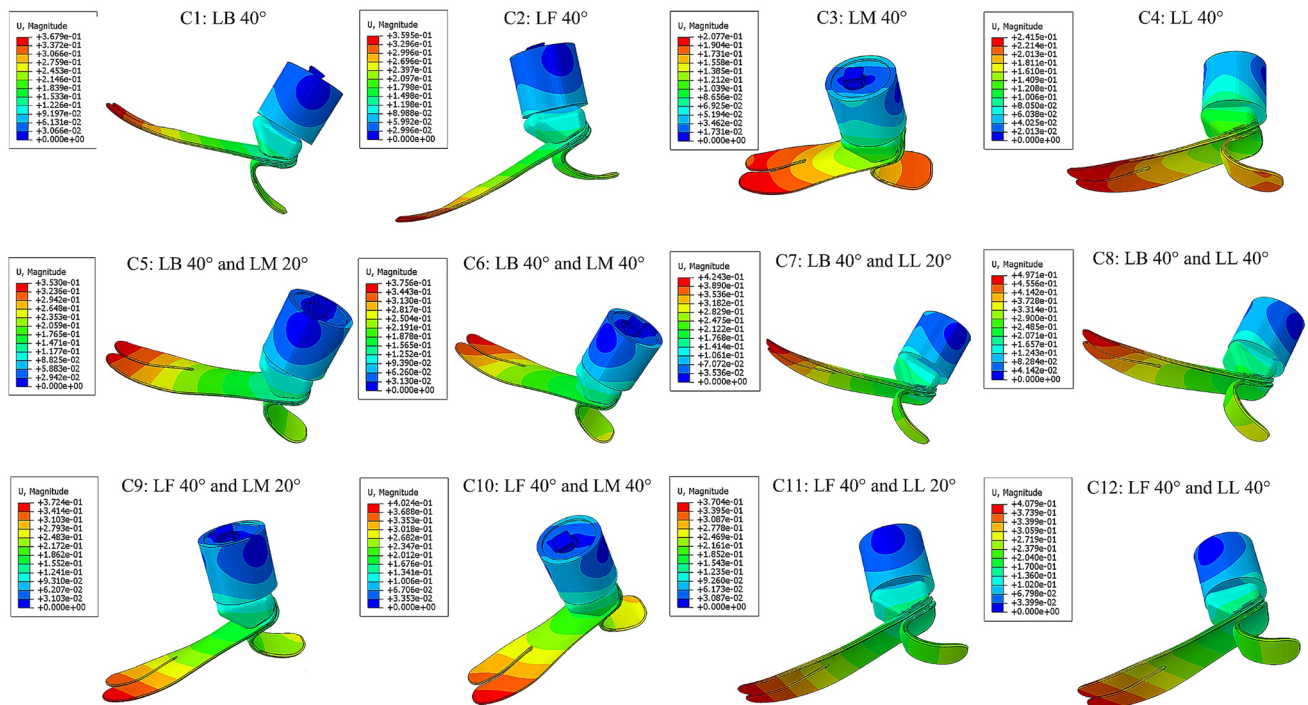


Fig. 4 Distribution of spatial displacement in the prosthesis under different working conditions. C, abbreviation of the condition

Table 4 Maximum moments and corresponding rotation angles under 12 different working conditions

Conditions	1	2	3	4	5	6	7	8	9	10	11	12
Maximum moments [Nm]	18.0	18.3	17.6	17.9	17.8	18.0	18.2	18.0	17.6	18.2	17.9	18.1
Rotation angles [deg]	5.7	5.2	5.5	4.3	4.2	4.9	4.1	4.8	5.0	4.4	4.3	4.0

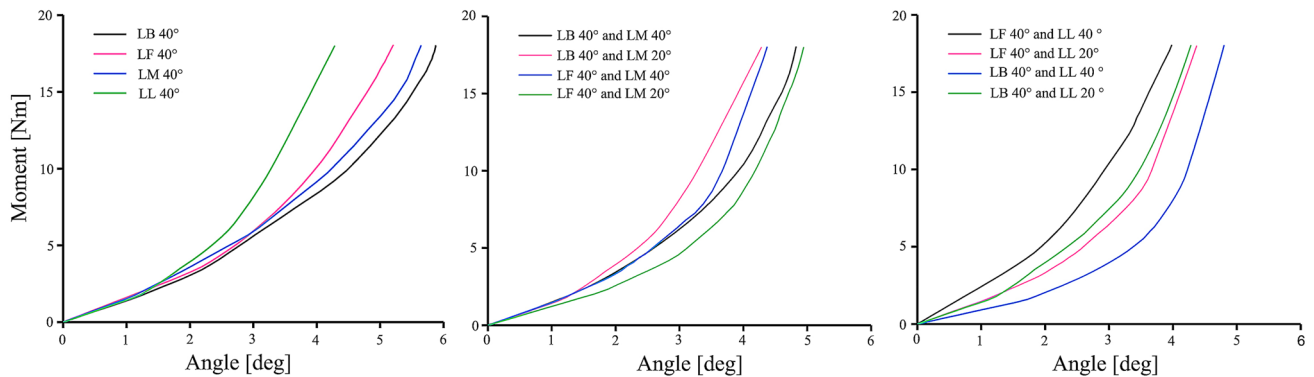


Fig. 5 Three-dimensional stiffness of the prosthetic ankle under 12 different working conditions

ankle characteristics as the 3D printed rigid components may maintain six DoFs (3 rotations and 3 translations) for the human ankle joint [36]. A flexible ankle prosthesis should conform to the nature of the walking gait of the amputee. The selection of soft materials is extremely important, as it is the key feature limiting bone movements. Proper soft material inclusions around the ankle can effectively stabilize

the ankle bones, withstand the multi-directional movements of the ankle, and provide a certain resilience to help store/release energy during walking.

FE analysis showed that the bionic prosthetic ankle had good variable stiffness in all directions. The functional rotation axis of the ankle was also consistent with the results from the literature, indicating that the bionic prosthesis can

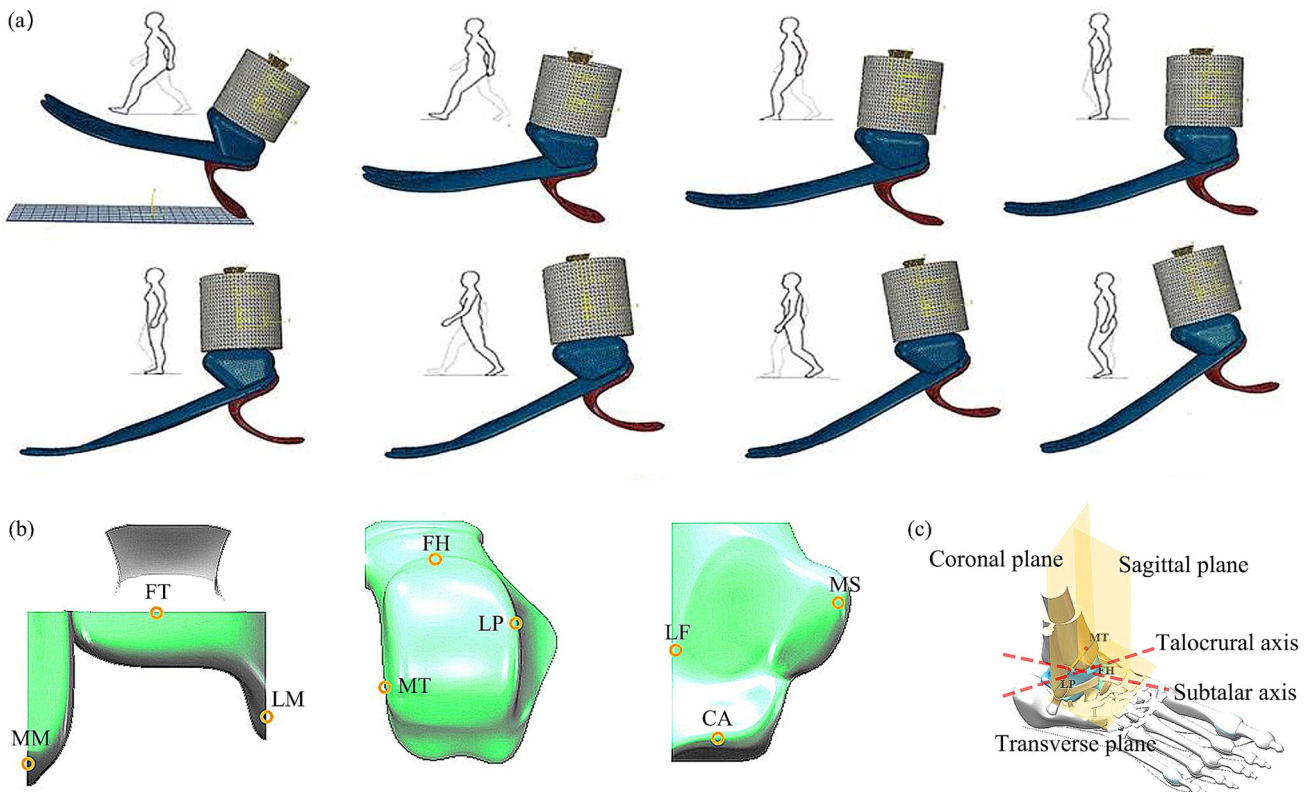


Fig. 6 Two rotation axes of the bionic prosthetic ankle. **a** Eight representative time points of walking. **b** Landmarks on different bone components. **c** Two joint axes in the foot coordinate frame

Table 5 Talocrural and subtalar axis angles compared with published literature data

Angle	Isman and Inman [32]	Inman [33]	Van den Bogert et al. [34]	Montefiori et al. [35]	This study
TaloInc	$80.0^{\circ} \pm 4.0^{\circ}$	$82.7^{\circ} \pm 3.7^{\circ}$	$85.4^{\circ} \pm 7.4^{\circ}$	$90.7^{\circ} \pm 4.1^{\circ}$	86.2°
TaloDev	$84.0^{\circ} \pm 7.0^{\circ}$	/	$89.0^{\circ} \pm 15.1^{\circ}$	$82.7^{\circ} \pm 7.4^{\circ}$	75.1°
SubInv	$41.0^{\circ} \pm 9.0^{\circ}$	$42^{\circ} \pm 9^{\circ}$	$35.3^{\circ} \pm 4.8^{\circ}$	$41.1^{\circ} \pm 14.1^{\circ}$	40.1°
SubDev	$23.0^{\circ} \pm 11.0^{\circ}$	$23^{\circ} \pm 11^{\circ}$	$18.0^{\circ} \pm 16.2^{\circ}$	$27.0^{\circ} \pm 9.0^{\circ}$	29.9°

Means \pm standard deviations are depicted for the data in the literature

help better restore the natural gait of the human body. The comparative analysis of kinematics and dynamics from gait measurements proved that the bionic flexible ankle prosthesis could simulate the natural gait mechanics of the healthy ankle in all three planes. Comparing the average value of the prosthesis with the data of the healthy side, the peak rotation angles in the sagittal plane at slow, normal and fast speeds were generally higher. The reason may have arisen from the inadequate mechanical properties of the soft materials, which led to excessive ankle motions during walking. In addition, at the early stance phase, the absolute value of ankle moment in the transverse plane on the prosthetic side was higher than that on the healthy side. This may be

because the subject could not well control the natural contact between the prosthesis and the ground, even received some adaptive trainings before the experiment. In addition, after several walking tests, some of the components were slightly loosened during walking, resulting in small displacement in the transverse plane.

Other researchers have also developed flexible passive prosthetic ankles with two or three DoFs that could partly achieve human-like ankle motions. For instance, a compliant passive ankle-foot prosthesis (CPAF) was designed on the basis of a parallel mechanism and soft rubbers [25], which could provide good gait movements and generate sufficient ankle moment when walking on level ground at

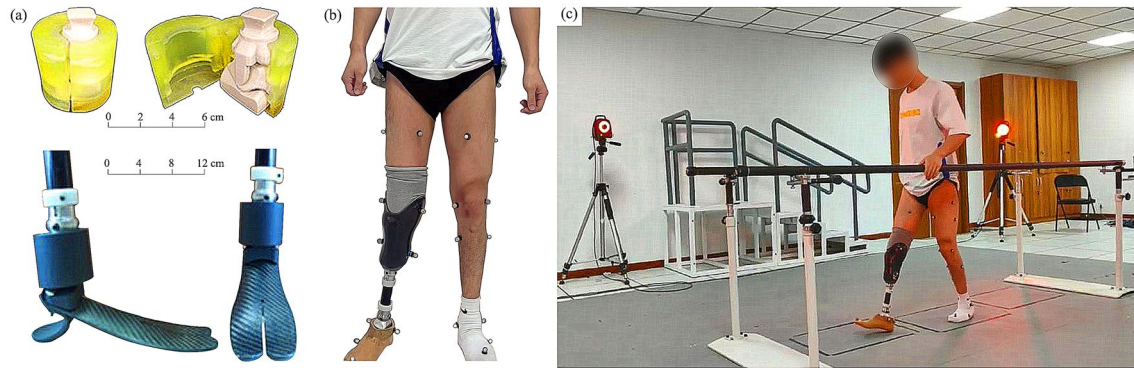


Fig. 7 Assembly of the prosthesis and validation by the subject with below-knee amputation. **a** Bionic prosthetic ankle and its connections to the foot plate and the leg tube. **b** Amputee wearing the bionic prosthesis. **c** Experimental setups

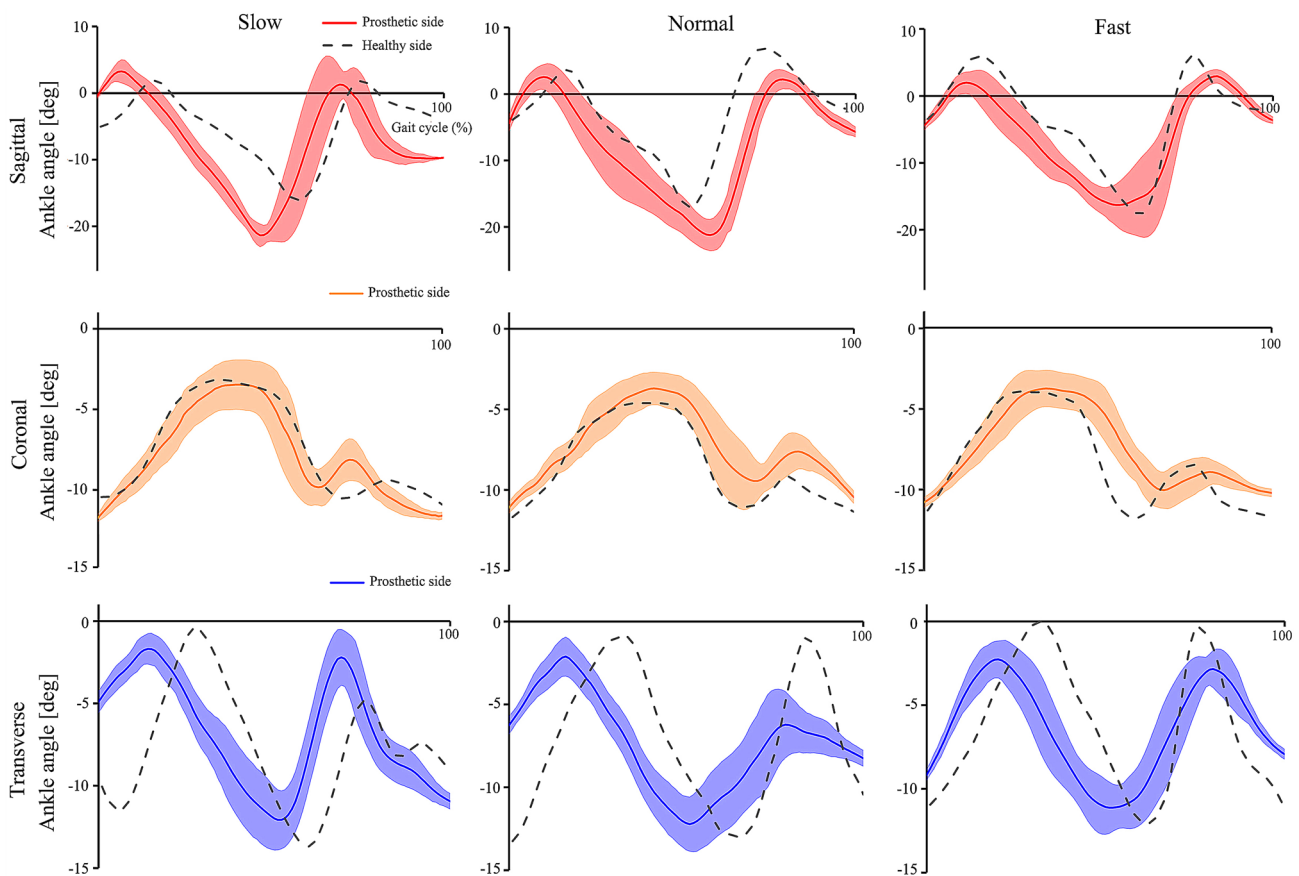


Fig. 8 Angles of the prosthetic ankle in three planes at different speeds

normal speed. Comparing the ankle moments of the flexible bionic ankle prosthesis with the CPAF in the three planes (Fig. 10), the peak values of the two prostheses in both sagittal and transverse planes were basically the same. Moreover, the peak moment of the bionic prosthesis in the coronal plane was lower than that of the CPAF. This benefit may have arisen from the soft material inclusions

around the bionic ankle mimicking the soft tissues of the human ankle, providing good deformation ability during the stance phase. This capability is not available in traditional rigid prostheses [37]. It should be noted that the time to reach the peak ankle moment of the CPAF on the sagittal plane was relatively delayed, while this time for the transverse plane was slightly early. In conclusion, the

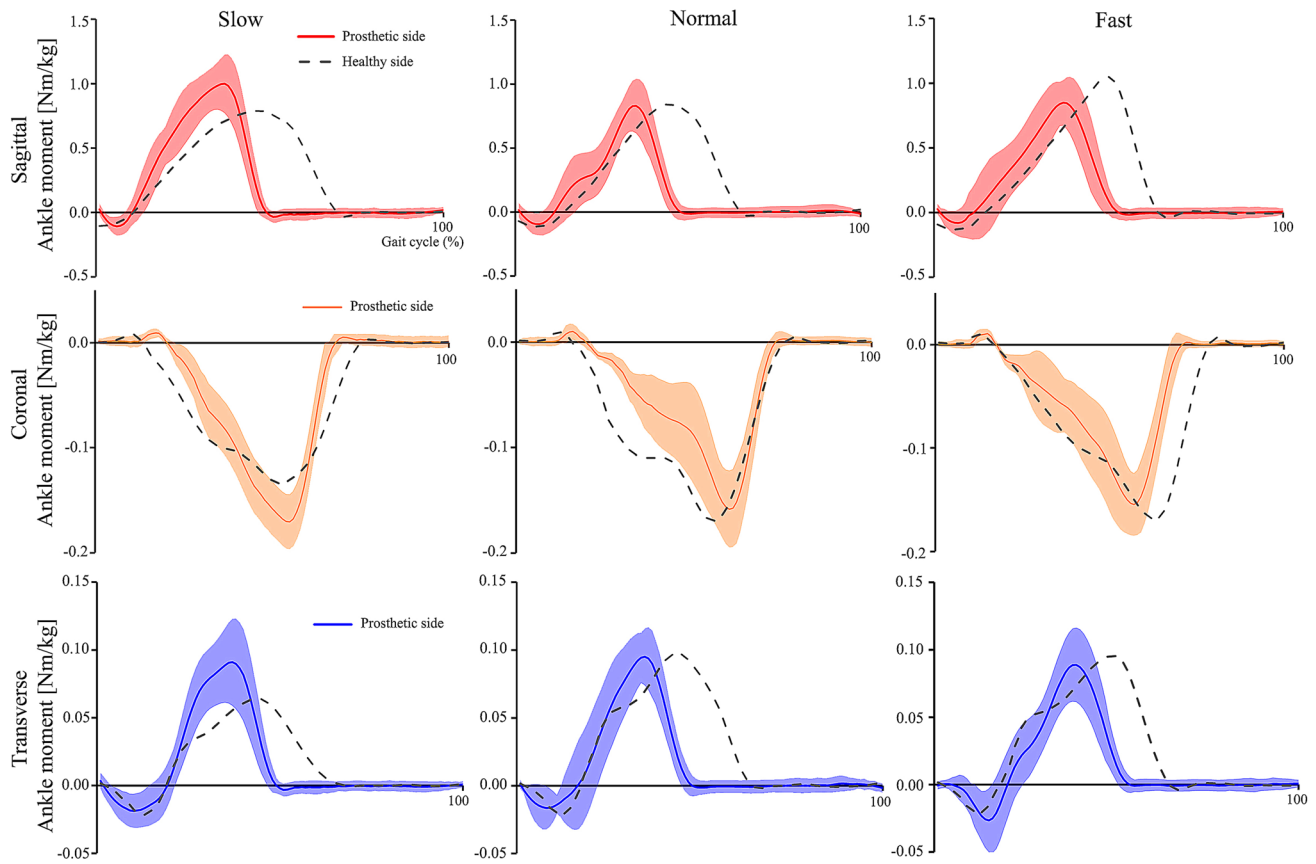


Fig. 9 Moments of the prosthetic ankle in three planes at different speeds

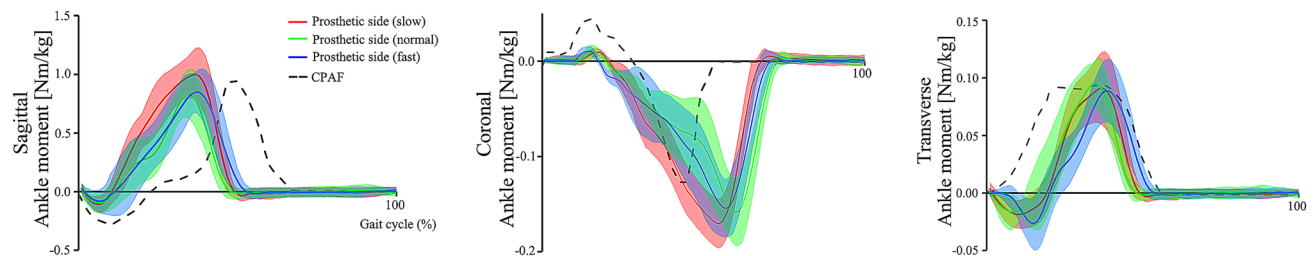


Fig. 10 Comparative analysis of ankle moments toward a CPAF ankle prosthesis [25]

flexible bionic ankle prosthesis had similar gait mechanics to the CPAF, suggesting that both prostheses could effectively assist walking with no activation.

In the future, we will continue to optimize the selection of proper soft materials covering the bionic prosthetic ankles. To facilitate manufacturing and reduce cost, the configuration of the bone components in the prosthesis should be simplified without reducing dynamic performance. More gait measurements with below-knee amputees should be carried out to provide adequate data analysis.

5 Conclusions

This study developed a flexible bionic ankle prosthesis based on subject-specific modeling of the human musculoskeletal system of a below-knee amputee. Soft material inclusions formed from polyurethane rubbers were designed to mimic the soft tissues of the human ankle, which could provide both stability and flexibility during different phases of walking. The bionic ankle had comparable dynamic properties with the human ankle in terms

of 3D variable stiffness under different external conditions and two rotating axes of the talocrural joint and subtalar joint during walking. This could yield great adaptation to the changes of different road conditions during daily lives. Gait analysis by the same subject wearing the prosthesis proved that the bionic ankle could simulate the natural gait mechanics of the healthy side, mainly including the ankle angles and moments in all three planes (sagittal, coronal and transverse) during walking. The bionic prosthesis has certain advantages in weight because it is mainly made of polyurethane materials. In addition, the subject-specific modeling for the reconstruction of the human musculoskeletal system can be used to customize prostheses for different amputees in accordance with their unique gait mechanics, which is not available with conventional prostheses. This study could provide a novel framework for the development of bionic prosthetic limbs.

Acknowledgements This research was partly supported by the National Key Research and Development Program of China (No. 2018YFC2001300), the National Natural Science Foundation of China (No. 52005209, 91948302, No. 91848204, No. 52021003), and the Natural Science Foundation of Jilin Province (No. 20210101053JC, No.20220508130RC).

Availability of Data and Materials The datasets generated during and/or analyzed during the current study are available from the corresponding author on reasonable request.

Declarations

Conflict of Interest The authors declare that they have no competing interest.

Open Access This article is licensed under a Creative Commons Attribution 4.0 International License, which permits use, sharing, adaptation, distribution and reproduction in any medium or format, as long as you give appropriate credit to the original author(s) and the source, provide a link to the Creative Commons licence, and indicate if changes were made. The images or other third party material in this article are included in the article's Creative Commons licence, unless indicated otherwise in a credit line to the material. If material is not included in the article's Creative Commons licence and your intended use is not permitted by statutory regulation or exceeds the permitted use, you will need to obtain permission directly from the copyright holder. To view a copy of this licence, visit <http://creativecommons.org/licenses/by/4.0/>.

References

- Ziegler-Graham, K., MacKenzie, E. J., Ephraim, P. L., Trivison, T. G., & Brookmeyer, R. (2008). Estimating the prevalence of limb loss in the United States: 2005 to 2050. *Archives of Physical Medicine and Rehabilitation*, 89(3), 422–429.
- Lauwers, P., Wouters, K., Vanoverloop, J., Avalosse, H., Hendriks, J., Nobels, F., & Dirinck, E. (2022). Temporal trends in major, minor and recurrent lower extremity amputations in people with and without diabetes in Belgium from 2009 to 2018. *Diabetes Research and Clinical Practice*, 189, 109972.
- Liu, J., Abu Osman, N. A., Al Kouzbary, M., Al Kouzbary, H., Abd Razak, N. A., Shasmin, H. N., & Arifin, N. (2021). Classification and comparison of mechanical design of powered ankle-foot prostheses for transtibial amputees developed in the 21st century: A systematic review. *Journal of Medical Devices*, 15(1), 010801.
- Lamers, E. P., Eveld, M. E., & Zelik, K. E. (2019). Subject-specific responses to an adaptive ankle prosthesis during incline walking. *Journal of Biomechanics*, 95, 109273.
- Segal, A. D., Zelik, K. E., Klute, G. K., Morgenroth, D. C., Hahn, M. E., Orendurff, M. S., Adamczyk, P. G., Collins, S. H., Kuo, A. D., & Czerniecki, J. M. (2012). The effects of a controlled energy storage and return prototype prosthetic foot on transtibial amputee ambulation. *Human Movement Science*, 31(4), 918–931.
- Dao, T. P., & Huang, S. C. (2015). Design, fabrication, and predictive model of a 1-dof translational flexible bearing for high precision mechanism. *Transactions of the Canadian Society for Mechanical Engineering*, 39(3), 419–429.
- Dao, T. P., & Huang, S. C. (2017). Optimization of a two degrees of freedom compliant mechanism using Taguchi method-based grey relational analysis. *Microsystem Technologies*, 23(10), 1–16.
- Ho, N. L., Dao, T. P., Huang, S. C., & Le, H. G. (2017). Design and optimization for a compliant gripper with force regulation mechanism. *International Journal of Aerospace and Mechanical Engineering*, 10(12), 1913–1919.
- Nguyen, T. T., Le, H. G., Dao, T. P., & Huang, S. C. (2017). Evaluation of structural behaviour of a novel compliant prosthetic ankle-foot. In *2017 International Conference on Mechanical, System and Control Engineering (ICMSC)*, Saint Petersburg, Russia, pp. 58–62.
- Kim, M., Chen, T., Chen, T., & Collins, S. H. (2018). An ankle-foot prosthesis emulator with control of plantarflexion and inversion–eversion torque. *IEEE Transactions on Robotics*, 34(5), 1183–1194.
- Collins, S. H., & Kuo, A. D. (2010). Recycling energy to restore impaired ankle function during human walking. *PLoS ONE*, 5(2), e9307.
- Pham, H. T., Le, M. N., & Mai, V. T. (2016). A Novel Multi-Axis Compliant Prosthetic Ankle Foot to Support the Rehabilitation of Amputees. In *2016 3rd International Conference on Green Technology and Sustainable Development (GTSD)*, Kaohsiung, Taiwan, China, pp. 238–243.
- Pham, H. T., Nguyen, V. K., & Mai, V. T. (2014). Shape optimization and fabrication of a parametric curved segment prosthetic foot for amputee. *Journal of Science and Technology: Technical Universities*, 102, 89–95.
- Sam, M., Childress, D., Hansen, A., Meier, M., Lambla, S., Grahn, E., & Rolock, J. (2004). The “shape&roll” prosthetic foot: I. Design and development of appropriate technology for low-income countries. *Medicine, Conflict & Survival*, 20(4), 294–306.
- Sam, M., Hansen, A. H., & Childress, D. S. (2000). Mechanical characterization of prosthetic feet using a Prosthetic Foot Loading Apparatus. In *Proceedings of the 22nd annual international conference of the IEEE engineering in medicine and biology society, Chicago, IL, USA*, pp. 1968–1971.
- Piazza, C., Santina, C. D., Gasparri, G. M., Catalano, M. G., Grioli, G., Garabini, M., & Bicchi, A. (2016). Toward an adaptive foot for natural walking. In *2016 IEEE-RAS 16th International Conference on Humanoid Robots (Humanoids)*, Cancun, Mexico, pp. 1204–1210.
- Winter, D. A. (1983). Biomechanical motor patterns in normal walking. *Journal of Motor Behavior*, 15(4), 302–330.
- Schlafly, M., & Reed, K. B. (2020). Novel passive ankle-foot prosthesis mimics able-bodied ankle angles and ground reaction forces. *Clinical Biomechanics*, 72, 202–210.
- Asaka, K., & Okuzaki, H. (2014). *Soft Actuators*. Springer.

20. Chen, R., Huang, C., Ke, Q. F., He, C. L., Wang, H. S., & Mo, X. M. (2010). Preparation and characterization of coaxial electrospun thermoplastic polyurethane/collagen compound nanofibers for tissue engineering applications. *Colloids and Surfaces B: Biointerfaces*, 79(2), 315–325.
21. Webster, T. J., Waid, M. C., McKenzie, J. L., Price, R. L., & Ejiogor, J. U. (2003). Nano-biotechnology: Carbon nanofibres as improved neural and orthopaedic implants. *Nanotechnology*, 15(1), 48–54.
22. Pedicini, A., & Farris, R. J. (2003). Mechanical behavior of electrospun polyurethane. *Polymer*, 44(22), 6857–6862.
23. Venkadesan, M., Yawar, A., Eng, C. M., Dias, M. A., Singh, D. K., Tommasini, S. M., Haims, A. H., Bandi, M. M., & Mandre, S. (2020). Stiffness of the human foot and evolution of the transverse arch. *Nature*, 579(7797), 97–100.
24. Akrami, M., Qian, Z. H., Zou, Z., Howard, D., Nester, C. J., & Ren, L. (2018). Subject-specific finite element modelling of the human foot complex during walking: Sensitivity analysis of material properties, boundary and loading conditions. *Biomechanics and Modeling in Mechanobiology*, 17(2), 559–576.
25. Xiu, H. H., Han, Y., Wang, X., Zhang, Y., Liang, W., Wei, G. W., Ren, L., & Ren, L. Q. (2022). Design, development, and clinical validation of a two degrees of freedom compliant ankle-foot prosthesis based on a 4–4r parallel mechanism. *Mechanism and Machine Theory*, 172, 104818.
26. Winter, D. A., & Sienko, S. E. (1988). Biomechanics of below-knee amputee gait. *Journal of Biomechanics*, 21(5), 361–367.
27. Gamage, S. S. H. U., & Lasenby, J. (2002). New least squares solutions for estimating the average centre of rotation and the axis of rotation. *Journal of Biomechanics*, 35(1), 87–93.
28. Hu, Z. Q., Ren, L., Hu, D., Gao, Y. L., Wei, G. W., Qian, Z. H., & Wang, K. Y. (2021). Speed-related energy flow and joint function change during human walking. *Frontiers in Bioengineering and Biotechnology*, 9, 666428.
29. Angeloni, C., Cappozzo, A., Catani, F., & Leardini, A. (1993). Quantification of relative displacement of skin-and plate-mounted markers with respect to bones. *Journal of Biomechanics*, 26, 864.
30. Garling, E. H., Kaptein, B. L., Mertens, B., Barendregt, W., Veeger, H. E. J., Nelissen, R. G. H. H., & Valstar, E. R. (2007). Soft-tissue artefact assessment during step-up using fluoroscopy and skin-mounted markers. *Journal of Biomechanics*, 40, S18–S24.
31. Cappozzo, A., Catani, F., Croce, U. D., & Leardini, A. (1995). Position and orientation in space of bones during movement: Anatomical frame definition and determination. *Clinical Biomechanics*, 10(4), 171–178.
32. Isman, R. E., & Inman, V. T. (1969). Anthropometric studies of the human foot. *Bulletin of Prosthetics Research*, 97, 97–129.
33. Inman, V. T. (1976). *The joints of the ankle*. Lippincott Williams & Wilkins.
34. van den Bogert, A. J., Smith, G. D., & Nigg, B. M. (1994). In vivo determination of the anatomical axes of the ankle joint complex: An optimization approach. *Journal of Biomechanics*, 27(12), 1477–1488.
35. Montefiori, E., Modenese, L., Di Marco, R., Magni-Manzoni, S., Malattia, C., Petrarca, M., Ronchetti, A., de Horatio, L. T., van Dijkhuizen, P., & Wang, A. (2019). An image-based kinematic model of the tibiotalar and subtalar joints and its application to gait analysis in children with Juvenile Idiopathic Arthritis. *Journal of Biomechanics*, 85, 27–36.
36. Wang, K. Y., Ren, L., Qian, Z. H., Liu, J., Geng, T., & Ren, L. Q. (2021). Development of a 3D printed bipedal robot: Towards humanoid research platform to study human musculoskeletal biomechanics. *Journal of Bionic Engineering*, 18, 150–170.
37. Li, L. R., Wang, X. M., Meng, Q. L., Chen, C. L., Sun, J., & Yu, H. L. (2022). Intelligent knee prostheses: A systematic review of control strategies. *Journal of Bionic Engineering*, 19, 1242–1260.

Publisher's Note Springer Nature remains neutral with regard to jurisdictional claims in published maps and institutional affiliations.